Applied Catalysis B: Environmental 121–122 (2012) 148–153

Contents lists available at SciVerse ScienceDirect

Applied Catalysis B: Environmental

journal homepage: www.elsevier.com/locate/apcatb

Synthesis of porous platinum-ion-doped titanium dioxide and the photocatalytic degradation of 4-chlorophenol under visible light irradiation

Suzuko Yamazaki*, Yuhei Fujiwara, Shinya Yabuno, Kenta Adachi, Kensuke Honda

Division of Environmental Science and Engineering, Graduate School of Science and Engineering, Yamaguchi University, Yamaguchi 753-8512, Japan

ARTICLE INFO

Article history:
Received 24 November 2011
Received in revised form 16 March 2012
Accepted 27 March 2012
Available online 4 April 2012

Keywords:
Visible-light responsive photocatalyst
Titanium dioxide
Platinum-doping
Kinetics

ABSTRACT

Porous platinum-ion-doped TiO_2 (Pt-TiO_2) with BET surface area higher than 200 $m^2\ g^{-1}$ was prepared by using water as solvent and conducting dialysis in a sol–gel method and demonstrated to have superior photocatalytic activity for the photodegradation of 4-chlorophenol (4-CP) under both ultraviolet and visible light (VL) irradiation. During dialysis, 76.5% of Cl^- was removed and mesopores were formed in Pt-TiO_2. Measurements of pore-size distribution indicated a peak at ca. 3 nm after the calcination of Pt-TiO_2 at 200 °C. Optimal conditions to prepare Pt-TiO_2 acting under VL were 0.5 at.% as the Pt-doping content and 200 °C as the calcination temperature in the range of 200–500 °C. Kinetic studies were performed to clarify the effect of the amount of Pt-TiO_2, initial concentration of 4-CP, intensity and wavelength of the incident light, pH and temperature on the reaction rate and to obtain the rate law under VL irradiation. Formation of benzoquinone and hydroquinone as intermediates was observed. They were further photodegraded on Pt-TiO_2 and 90.7% of 4-CP was completely mineralized at the VL irradiation of 390 min.

© 2012 Elsevier B.V. All rights reserved.

1. Introduction

Photodegradation of various pollutants by photocatalysis using semiconductors has been widely studied over the last 30 years. Among them, the TiO_2 has been the most studied photocatalyst since it is stable, harmless and inexpensive and has a high reactivity for decomposition of harmful compounds [1–5]. However, TiO_2 is active only under ultraviolet (UV) irradiation ($\lambda < 388$ nm) due to its wide band gap energy of ca. 3.2 eV. Significant efforts have been made to extend the spectral response of TiO_2 to visible light (VL) [6]. In order to enhance the efficiency of the photocatalysis, it is important to develop modified TiO_2 that can operate efficiently under both UV and VL. Since Asahi et al. reported that TiO_2 doped with nitrogen exhibited VL-activity for the degradation of organic compounds, TiO_2 doped with nonmetallic elements such as carbon, sulfur, phosphorous and boron has been investigated for their photocatalysis under VL irradiation [7–11]. Among them, N-doped TiO_2 has been examined intensively and demonstrated to offer modest VL-activity to TiO_2 but lower the UV-activity [6,12,13]. Another approach is doping various transition-metal ions such as iron, vanadium, nickel and platinum into TiO_2 [14–18]. Choi and his coworkers synthesized Pt-ion-doped TiO_2 by a simple sol–gel method and investigated its properties and VL-activities for the degradation of chlorinated organic compounds such as 4-chlorophenol (4-CP) and dichloroacetate [18]. Their catalysts have Pt ions substituted in the TiO_2 lattice and higher photocatalytic activities than undoped TiO_2 under UV irradiation as well. Hoffman and his coworkers prepared TiO_2 doped with 13 different metal ions by the sol–gel method, characterized their physicochemical properties and described that Pt- or Cr-ion doping showed a significantly enhanced VL-activity [19,20].

In the sol–gel method, most metal oxide particles are charged at low pH and thus, they repel each other upon approach, forming a stable colloidal suspension. However, when the pH is increased by gradually removing protons from the suspension through dialysis, the particles tend to undergo aggregation, leading to the formation of large pores. Xu and Anderson reported that porosity and specific surface area of TiO_2 xerogel prepared by the sol–gel method increased with an increase in pH of the sol by dialysis [21]. We have prepared highly porous TiO_2 pellets according to their method and demonstrated the high photocatalytic activity for the photodegradation of gaseous contaminants such as chlorinated ethylenes and ethanes under UV irradiation [22–25]. In this paper, we prepared porous Pt-ion-doped TiO_2 (Pt-TiO_2) by the modified sol–gel method incorporating the dialysis process and investigated the photocatalytic activity for the degradation of 4-CP.

2. Experimental

2.1. Preparation of photocatalyst

Approximately 15 ml of $Ti(OC_3H_7)_4$ was added dropwise to 180 ml of aqueous solutions containing 1.3 ml of HNO_3 and hydrogen hexachloroplatinate(IV) hexahydrate (typically 0.13 g for

* Corresponding author. Tel.: +81 83 933 5763; fax: +81 83 933 5763.
E-mail address: yamazaki@yamaguchi-u.ac.jp (S. Yamazaki).

0926-3373/$ – see front matter © 2012 Elsevier B.V. All rights reserved.
http://dx.doi.org/10.1016/j.apcatb.2012.03.026

0.5 at.% Pt doping). The obtained mixture was peptized at room temperature for 6 days to form a highly dispersed colloidal solution. This sol was then dialyzed in a molecularly porous dialysis tube (molecular weight cut-off: 3500) for 3 days until approximately pH 4 was obtained. The sol was dried in an oven at 40 °C for 3 days and the resulting gel was calcined at 200–500 °C (ramping rate at 3 °C min^{-1} and keeping the desired temperature for 2 h). The orange xerogel was crushed into powders by using mortar and pestle. Undoped TiO_2 powder was prepared according to the above procedures without addition of hydrogen hexachloroplatinate(IV) hexahydrate. Commercial TiO_2 powder (Degussa P-25) was also used for comparison.

Concentration of Cl^- or NO_3^- in water during the dialysis was analyzed by ion chromatography (Shimadzu, PIA-1000) and that of Pt ion was determined by inductively coupled plasma spectroscopy (Varian, ICP-AES Liberty Series II).

2.2. Characterization of catalyst

X-ray diffraction (XRD, Rikagaku RINT-2500) analysis was performed with Cu Kα radiation (40 kV, 100 mA) at 2θ angles from 10° to 90° with a scan speed of 4° min^{-1}. The Brunauer–Emmett–Teller (BET) surface area was measured with nitrogen as the adsorptive gas by automatic surface area analyzer (Shimadzu, Gemini 2370 and 2390). Diffuse reflectance UV–vis absorption spectra of the powder samples were obtained using a spectrophotometer (Nippon Bunko, V-670). Measurements of diffuse reflectance infrared Fourier transform (DRIFT) spectra were performed by utilizing a FTIR spectrophotometer (Nicolet AVATAR 370 DTGS) equipped with a DRIFT accessory (AVATAR Collector II).

2.3. Photocatalytic degradation of 4-CP

An aqueous suspension containing 4-CP and Pt-TiO_2 was placed into a Pyrex bottle which was immersed in a thermostated water bath on a magnetic stirrer. After air was purged through the suspension for 30 min under vigorously stirring, a 150 W halogen lamp was ignited. The light intensity through a long pass filter (Edmund, cut-on wavelength: 400 nm), which was measured at the center of the Pyrex bottle was 63 mW cm^{-2} (Koito, memory sensor MES-101 with IKS-37). Samples of 8 ml were withdrawn from the suspension at appropriate times and centrifuged at 2000 rpm for 15 min. The supernatant liquid was filtrated through a 0.45 μm filter and then analyzed by a high performance liquid chromatograph (HPLC, Shimadzu) equipped with a UV–vis detector and a C18 column (Shim-pack, VP-ODS 4.6 mm × 25 cm). The eluent was a mixture of water with methanol (1:1 by volume). Mineralization was determined by using total organic carbon analyzer (Shimadzu, TOC 5000A) and by-products were identified with gas chromatograph/mass spectrometer (Shimadzu, GC/MS QP2010). For comparison, photocatalytic experiments were performed by using four 4 W black-lights as UV light source. The light intensity was measured to be 3.5 mW cm^{-2} by radio meter (Iuchi, UVR-400, S-365).

3. Results and discussion

3.1. Photocatalytic activity under UV and VL irradiation

Fig. 1 indicates that photocatalytic activity of Pt-TiO_2 is much higher than that of TiO_2 under both UV and VL irradiation. Conversions of 4-CP on Pt-TiO_2 and TiO_2 were 99.8% and 37.3%, respectively, at the UV irradiation for 60 min and those are 82.0% and 11.3% at the VL irradiation for 60 min. The BET surface area was measured to be 263 and 236 m^2 g^{-1} for Pt-TiO_2 and TiO_2, respectively. Since these values nearly equal, the difference in the activity

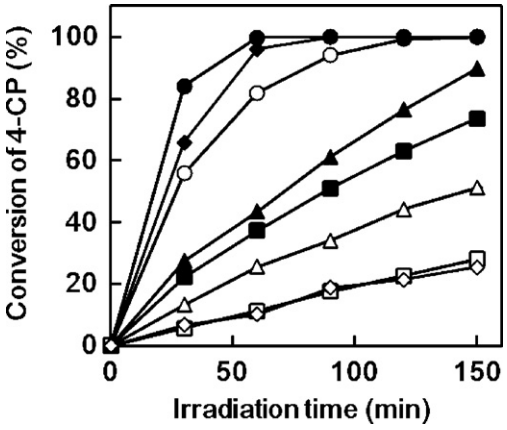

Fig. 1. Time course of 4-CP conversion on Pt-TiO_2, Pt-TiO_2(ref) and TiO_2 which were calcined at 200 °C and on commercial TiO_2 (P-25). Reaction conditions were 1.0×10^{-4} mol dm^{-3} 4-CP aqueous solution suspended with 0.2 wt% photocatalysts at 30 °C. Under UV: Pt-TiO_2 (●), Pt-TiO_2(ref) (▲), TiO_2 (■), P-25 (♦); under VL: Pt-TiO_2 (○), Pt-TiO_2(ref) (△), TiO_2 (□), P-25 (◊).

can be ascribed to the doping of Pt ion. Higher VL-activity of Pt-TiO_2 is attributable to the higher absorption ability induced by the Pt doping since the color of Pt-TiO_2 is yellow. On the other hand, higher activity under UV illumination is ascribed to the suppression of the recombination between photogenerated holes and electrons by doping Pt ion [26].

3.2. Comparison of photocatalytic activity with another Pt-TiO_2

For comparison, Pt-TiO_2 was prepared by the method reported by Choi and his coworkers (hereafter, Pt-TiO_2(ref)) [18]. In their method, the Pt-TiO_2(ref) was prepared by stirring the mixture of $Ti(OC_3H_7)_4$, H_2PtCl_6 and HNO_3 in ethanol–water (1:10) solvent, followed by evaporation, dryness and calcination. During the process of drying, a corrosive gas (probably HCl) was evolved to corrode the stainless steel oven. On the other hand, in our method, only water was used as the solvent and chloride ion was removed during the dialysis. Thus, our method is more environmentally benign. Besides, the photocatalytic activity of our Pt-TiO_2 was much higher than Pt-TiO_2(ref) under both UV and VL irradiation as shown in Fig. 1. The reason was attributable to the fact that the surface area of the Pt-TiO_2(ref) was estimated to be 131 m^2 g^{-1} which was lower by a factor of 0.5 than our Pt-TiO_2. Fig. 1 also indicates that our Pt-TiO_2 is more active than the commercial TiO_2 powder (P-25) which is used widely in the field of photocatalytic reactions under UV irradiation.

The nitrogen adsorption–desorption isotherm of Pt-TiO_2 exhibited a hysteresis loop at the relative pressure ranges of 0.4–0.6, which was associated with the filling and emptying of mesopores by capillary condensation. As shown in Fig. 2, the pore size distribution of Pt-TiO_2 indicated the peak at ca. 3 nm as mesopores but no peak was observed with Pt-TiO_2(ref) in the mesopore region. During dialysis, the pH of the sol gradually increased towards the isoelectric point of TiO_2 nanoparticles with the loss of net surface charges. Such reduction in net surface charges would result in decreased electrostatic repulsion of the particles to form mesopore. Anderson and his coworkers described that the BET surface area and porosities of MnO_2 xerogels increased by conducting dialysis in sol–gel method [27]. Therefore, the dialysis process leads to the formation of porous Pt-TiO_2 with the high BET surface area as well as the removal of Cl^-. Fig. 3 depicts the removal of Cl^-, NO_3^- and Pt ion from the sol during the dialysis. The removal percent of Cl^-, NO_3^- or Pt ion was calculated to be 64.6, 65.0 or 1.86%, respectively, at the first dialysis and decreased by exchanging water. The

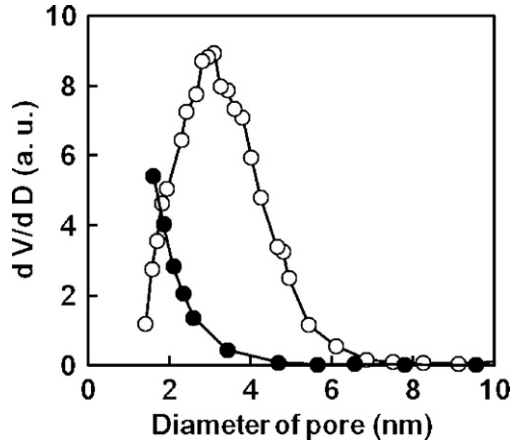

Fig. 2. Pore size distribution of Pt-TiO_2 (○) and Pt-TiO_2(ref) (●) after being calcined at 200 °C.

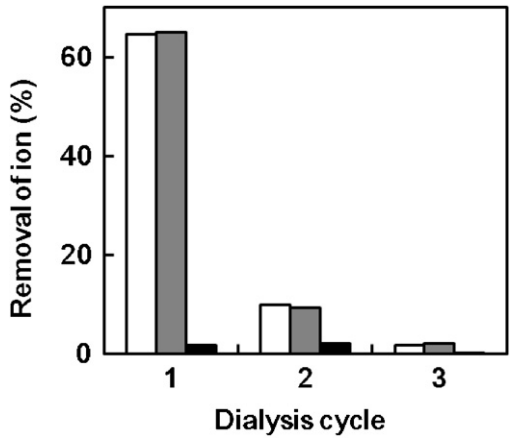

Fig. 3. Removal percent of Cl^- (□), NO_3^- (■) and Pt (■) ion during dialysis.

formation of Cl^- ion is caused by hydrolysis of $PtCl_6^{2-}$ [28]. It is worthy to note that 76.5% of Cl^- and 76.6% of NO_3^- were removed by conducting the dialysis three times whereas only 4.1% of Pt ion was removed. Such a low removal supports the fact that Pt ion was doped efficiently in TiO_2, which might be due to the ionic radius of Pt^{4+} (0.765 Å) similar to Ti^{4+} (0.745 Å) [29]. More studies are required to clarify the Pt-doping mechanism via hydrolysis of $PtCl_6^{2-}$.

3.3. Effect of doping amount of Pt and calcination temperature

Crystalline size, band gap and the BET surface area for Pt-TiO_2 prepared under various conditions are listed in Tables 1 and 2. Crystalline size means the diameter of anatase crystals estimated by using Scherrer equation. Band gap energy was evaluated from Tauc plots. Table 1 indicates that band gap becomes narrow and BET surface area increases as the Pt-doping amount increases up to 1.0 at.%. The changes in the band gap indicate that the doping of Pt ion lowers the conduction band edge. Such a shift in the conduction band edge was described for Pt-TiO_2(ref) by Choi et al. because they observed the positive shift by 50 mV in the flat band potentials of Pt-TiO_2(ref) compared with TiO_2. The XRD patterns attributable only to anatase were observed on the Pt-TiO_2 calcined at 200 °C irrespective of the doping amount in the range of 0–1.0 at.%. Fig. 4 shows the 4-CP conversion is almost the same on the Pt-TiO_2 above 0.5 at.% Pt.

Table 1
Effect of amount of Pt on crystalline size, band gap and BET surface area of Pt-TiO_2.[a]

Amount of Pt (at.%)	Crystalline size (nm)	Band gap (eV)	BET surface area ($m^2\,g^{-1}$)
0	4.3	3.1	236
0.2	4.4	3.0	266
0.5	4.3	2.9	273
0.8	3.8	2.8	296
1.0	3.9	2.8	287

[a] Pt-TiO_2 was calcined at 200 °C.

Table 2
Effect of calcination temperature on crystalline size, band gap and BET surface area of Pt-TiO_2.

Calcination temp.(°C)	Crystalline size (nm)	Band gap (eV)	BET surface area ($m^2\,g^{-1}$)
200	4.3	2.9	273
300	5.5	2.8	196
400	7.0	2.7	147
500	10.1	2.6	60.3

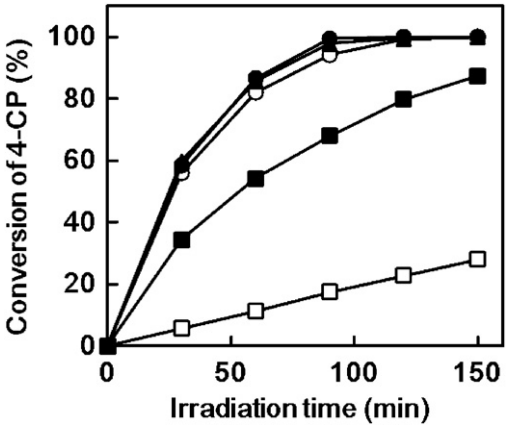

Fig. 4. Time course of 4-CP conversion on Pt-TiO_2 whose Pt contents were 0 (□), 0.2 (■), 0.5 (○), 0.8 (▲) and 1.0 (●) at.%. Reaction conditions were the same as in Fig. 1.

The XRD patterns of the Pt-TiO_2 (0.5 at.% Pt) calcined at 200–500 °C indicate that the anatase phase is predominant up to 400 °C and the intense peaks due to rutile were appeared at 500 °C as shown in Fig. 5. Table 2 presents that the band gap decreased from 2.9 to 2.6 eV and the BET surface area decreased from 273 to 60.3 $m^2\,g^{-1}$ as the calcination temperature increased from 200 to 500 °C. These findings suggest that the absorption ability to the visible light is the highest at 500 °C although the BET surface area at 500 °C is the lowest. Fig. 6 depicts that the 4-CP conversion decreases as the calcination temperature increases. The 4-CP

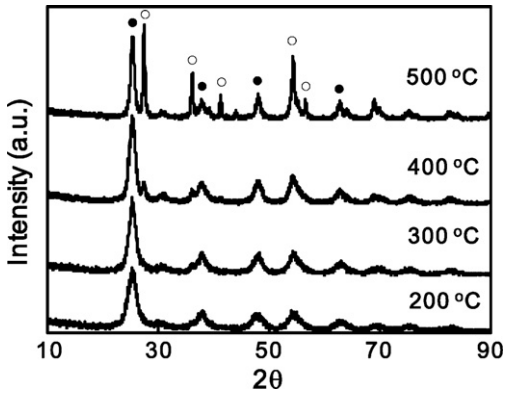

Fig. 5. XRD patterns of Pt-TiO_2 (0.5 at.% Pt) calcined at 200–500 °C. Anatase (●), rutile (○).

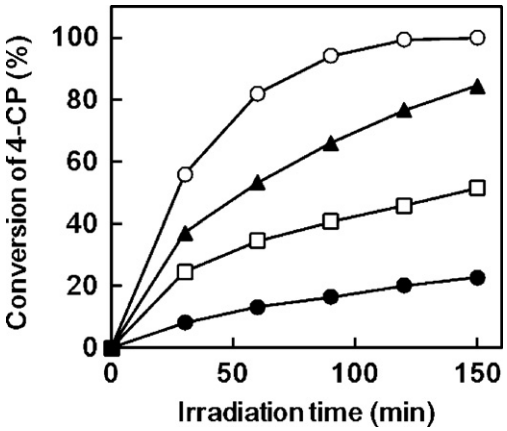

Fig. 6. Time course of 4-CP conversion on Pt-TiO_2 calcined at 200 (○), 300 (▲), 400 (□) and 500 °C (●). Reaction conditions were the same as in Fig. 1.

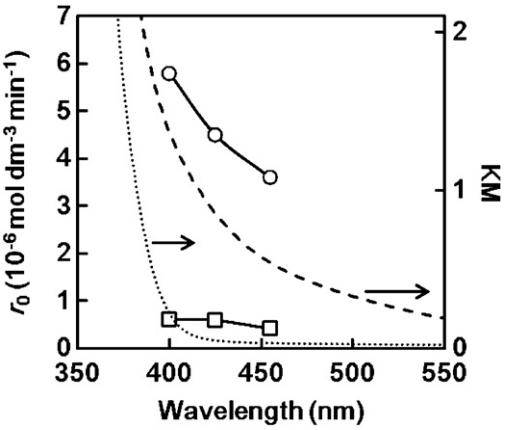

Fig. 8. Dependence of r_0 on the cut-on wavelength of the long pass filter (400, 420, 455 nm) and diffuse reflectance spectra of Pt-TiO_2 (○, broken line) and TiO_2 (□, dotted line). Reaction conditions were the same as in Fig. 1 except for 1.0×10^{-3} mol dm^{-3} 4-CP.

conversions at the irradiation for 2 h were evaluated to be 99.4, 76.6, 45.7 and 20.1% on Pt-TiO_2 calcined at 200, 300, 400 and 500 °C, respectively. This tendency can be explained in terms of the remarkable decrease in the BET surface area at higher calcination temperature. The Pt-TiO_2 with 0.5 at.% Pt and calcined at 200 °C was used for kinetic studies described below.

3.4. Effect of reaction conditions on the reaction rate

The concentration of 4-CP in the reaction solution was analyzed every 5 min from the start of the light irradiation under various conditions. The initial reaction rate (r_0) was evaluated from the initial slope of the concentration of 4-CP vs. the irradiation time. Fig. 7 indicates that r_0 increases with an increase in the amount of the Pt-TiO_2 suspended and tends to approach a constant value. Fig. 8 shows the dependence of r_0 on the cut-on wavelength (λ_c) of the long pass filter which was used for the light irradiation and the diffuse reflectance spectra of Pt-TiO_2 and TiO_2 as prepared. The r_0 values decrease from 5.8×10^{-6} mol dm^{-3} min^{-1} to 3.6×10^{-6} mol dm^{-3} min^{-1} as the λ_c increases from 400 to 455 nm, which corresponds to the decrease in the absorption of Pt-TiO_2. It is worthy to note that 4-CP is degraded even at the irradiation wavelength longer than 455 nm although the r_0 value decreased by a factor of 0.62 of that at λ_c = 400 nm. In general, the band gap of TiO_2 is 3.0–3.2 eV, meaning that it is inactive under VL illumination. Fig. 8 also indicates that 4-CP is degraded on TiO_2, for which the r_0 values are lower by one order of magnitude than those on Pt-TiO_2. Some studies reported that the surface complexation between phenolic compounds and TiO_2 caused the visible light absorption which induced the photocatalytic conversion of substrate [30]. In this study, Pt-TiO_2 itself shows light absorption in the visible region and no appreciable difference in the diffuse reflectance spectra was observed for Pt-TiO_2 powders with and without adsorbing 4-CP. The r_0 values observed on Pt-TiO_2 are much higher than those on TiO_2 although their surface areas are not so different, i.e. 273 and 236 m^2 g^{-1}, respectively. Thus, the degradation of 4-CP via the light absorption of the surface complex with Pt-TiO_2 is negligible.

Fig. 9 shows the dependence of r_0 on the initial concentration of 4-CP ($[4\text{-CP}]_0$) and the inset indicates that a linear relationship with an intercept is obtained when the reciprocal of r_0 is plotted against that of $[4\text{-CP}]_0$. Fig. 10 depicts the dependence of r_0 on pH of the reaction solution. The r_0 values were evaluated to be almost the same at pH 3.3 and 4.5 and decreased remarkably at pH above 8.5. This pH dependence corresponds well with that of the fraction of nondissociated 4-CP, which is calculated from the acid dissociation constant of 4-CP (pK_a = 9.4). This finding indicates that it is not the deprotonated but the nondissociated 4-CP to be degraded on Pt-TiO_2. The deprotonated 4-CP with a negative charge cannot adsorb on the TiO_2 at pH higher than the isoelectric point (ca. 6), where the TiO_2 surface is charged negatively. Fig. 11 shows that r_0 increases with an increase in the light intensity (I_0) and approached a maximal value which is estimated to be 5.68×10^{-6} mol dm^{-3} min^{-1} by fitting the experimental data. It is noted that the r_0 value obtained

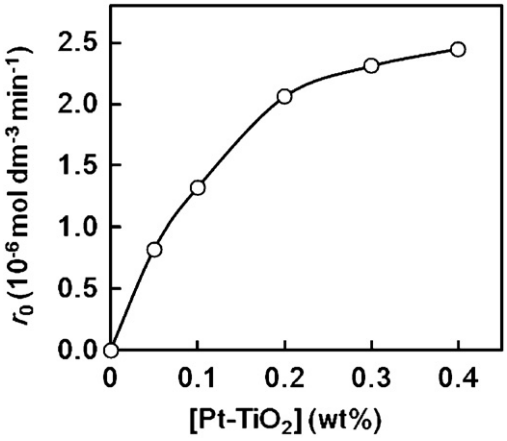

Fig. 7. Dependence of r_0 on the amount of Pt-TiO_2 suspended in the reaction solution. Reaction conditions were the same as in Fig. 1.

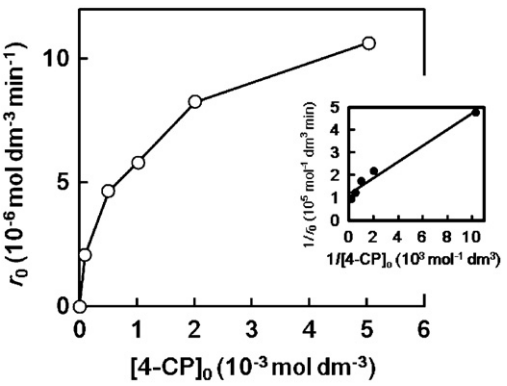

Fig. 9. Effect of initial concentration of 4-CP on r_0. The inset is the plot of the reciprocal of r_0 against that of the initial concentration of 4-CP.

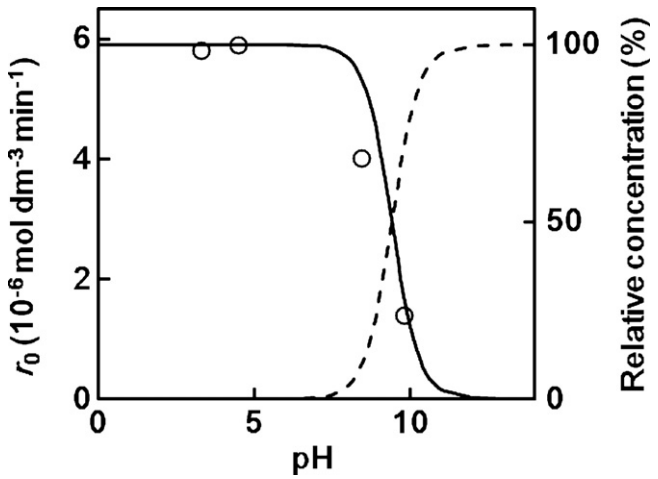

Fig. 10. Effect of pH on r_0 and relative concentration of 4-CP (solid line) and deprotonated 4-CP (broken line). Reaction conditions were the same as in Fig. 8.

at 63 mW cm^{-2} which is the standard condition used in this study is almost the same as the maximum. The slope of the plots of log r_0 vs. log I_0 was calculated to be 0.56, suggesting that the reaction order with respect to the incident light intensity is 0.56.

The formation of surface complex of TiO_2 with phenolic compounds such as 4-CP, 2,4-dichlorophenol, and catechol has been reported [30–32]. Orlov et al. studied interactions of 4-CP with TiO_2 under well-defined UHV conditions by means of EXAFS, time-dependent XPS, and UPS and described that 4-CP was adsorbed on TiO_2 via a phenolate link with a coverage-dependent tilted geometry to form a surface 4-CP/TiO_2 complex [33]. Diffuse reflectance FTIR was measured with 4-CP mixed with KBr, Pt-TiO_2 and Pt-TiO_2 adsorbed with 4-CP. The last sample was prepared by immersing Pt-TiO_2 into 0.01 mol dm^{-3} 4-CP aqueous solution followed by filtration and drying. By adsorbing 4-CP on Pt-TiO_2, peaks at 1435 and 1358 nm which are assigned to O—H in-plane bending in 4-CP were disappeared and a peak at 1238 nm due to C—O stretching vibration was shifted to 1271 nm. The disappearance of the OH bending mode of 4-CP and a shift in the C—O stretching frequency is in good accord with the observation with TiO_2 adsorbed with 4-CP [31,33]. These findings indicate the bonding of 4-CP with Pt-TiO_2 by a phenolate link.

Some research groups described that the addition of an excess of tert-butyl alcohol (TBA) significantly reduced the photocatalytic degradation rate of 4-CP under UV irradiation since TBA acted as an OH radical scavenger [18,34]. In the present study, no appreciable difference in r_0 was observed with and without the addition of TBA. Thus, the adsorbed 4-CP seems to be degraded not by OH radicals but by the photogenerated holes.

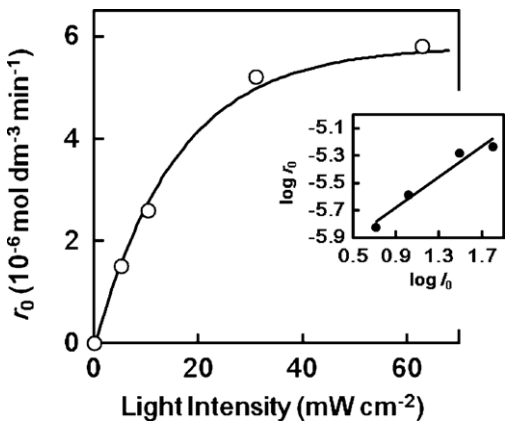

Fig. 11. Effect of light intensity on r_0. The inset is the plot of logarithm of r_0 against that of intensity of the incident light. Reaction conditions were the same as in Fig. 8.

3.5. Rate law

On the basis of the kinetic data, the following reaction scheme can be postulated where S_v and I_a denote the vacant sites for the formation of the adsorbed 4-CP (4-CP(a)) and the light intensity absorbed by Pt-TiO_2, respectively.

$$4\text{-CP} + S_v \underset{k_d}{\overset{k_a}{\rightleftarrows}} 4\text{-CP(a)} \quad (1)$$

$$\text{Pt-TiO}_2 + h\nu \xrightarrow{I_a} e^- + h^+ \quad (2)$$

$$e^- + h^+ \xrightarrow{k_r} \text{recombination} \quad (3)$$

$$e^- + O_2(a) \xrightarrow{k_e} O_2^- \quad (4)$$

$$h^+ + 4\text{-CP(a)} \xrightarrow{k_h} (4\text{-CP})^+ \quad (5)$$

From these reactions, the reaction rate ($-d$[4-CP]/dt) is obtained as follows.

$$-\frac{d[4\text{-CP}]}{dt} = k_a[4\text{-CP}][S_v] - k_d[4\text{-CP(a)}] \quad (6)$$

If we assume the steady state concentrations for the 4-CP(a) and the photogenerated holes and electrons, the following equations are obtained.

$$\frac{d[4\text{-CP(a)}]}{dt} = -k_h[h^+][4\text{-CP(a)}] + k_a[4\text{-CP}][S_v] - k_d[4\text{-CP(a)}] = 0 \quad (7)$$

$$\frac{d[h^+]}{dt} = I_a - k_r[e^-][h^+] - k_h[h^+][4\text{-CP(a)}] = 0 \quad (8)$$

$$\frac{d[e^-]}{dt} = I_a - k_r[e^-][h^+] - k_e[e^-][O_2(a)] = 0 \quad (9)$$

As mentioned above, the r_0 value was almost the same as the maximum under the light irradiation of 63 mW cm^{-2} which was used as the standard condition. This means that most of the photogenerated holes and electrons are consumed by the recombination and thus, their concentrations are assumed to be equal. Then, Eq. (8) can be written as follows:

$$I_a - k_r[h^+]^2 - k_h[h^+][4\text{-CP(a)}] = 0 \quad (10)$$

Assuming that $k_r > k_h$ and [h^+] > [4-CP(a)], Eq. (11) is obtained.

$$[h^+] = \left(\frac{I_a}{k_r}\right)^{1/2} \quad (11)$$

Substitution of Eqs. (7) and (11) to Eq. (6) gives Eq. (12).

$$-\frac{d[4\text{-CP}]}{dt} = k_h(I_a/k_r)^{1/2}[4\text{-CP(a)}] \quad (12)$$

Considering the total surface sites (S_0) and the adsorption constant (K_{ads}) of 4-CP on the Pt-TiO_2 surface, Eq. (14) is obtained.

$$[S_v] + [4\text{-CP(a)}] = [S_0] \quad (13)$$

$$[4\text{-CP(a)}] = \frac{K_{ads}[4\text{-CP}][S_0]}{1 + K_{ads}[4\text{-CP}]} \quad (14)$$

Finally, substitution of Eq. (14) for (12) gives the following rate law.

$$-\frac{d[4\text{-CP}]}{dt} = \frac{k_{obsd}K_{ads}[4\text{-CP}]}{1 + K_{ads}[4\text{-CP}]} \quad (15)$$

Table 3
Effect of temperature on the values of k_{obsd} and K_{ads}.

Temp. (°C)	k_{obsd} (10^{-6} mol dm^{-3} min^{-1})	K_{ads} (10^{3} mol^{-1} dm^{3})
30	8.64	3.17
60	8.61	2.50

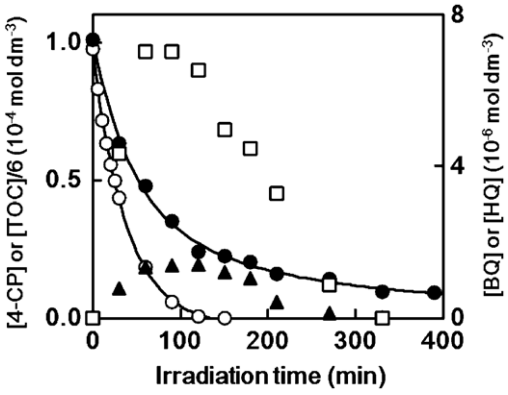

Fig. 12. Time course of the concentration of 4-CP (○), TOC (●), BQ (□) and HQ (▲). Reaction conditions were the same as in Fig. 1. The values of TOC were divided by 6 to compare with 4-CP in the same concentration range.

where k_{obsd} denotes $k_h(I_a/k_r)^{1/2}[S_0]$. At the initial period of the reaction,

$$r_0 = \frac{k_{obsd}K_{ads}[4\text{-CP}]_0}{1 + K_{ads}[4 - \text{CP}]_0} \quad (16)$$

Eq. (16) suggests that the r_0 value is proportional to $I_0^{0.5}$ since I_a is proportional to I_0 and that the plots of $1/r_0$ vs. $1/[4\text{-CP}]_0$ give a straight line with an intercept, both of which can satisfy the results presented in Figs. 11 and 9, respectively. Furthermore, Eq. (16) indicates that such plots have an intercept of $1/k_{obsd}(=(k_r/I_a)^{1/2}/(k_h[S_0]))$ and a slope of $1/(k_{obsd}K_{ads})$. Table 3 lists the values of k_{obsd} and K_{ads} which were calculated from the plots of $1/r_0$ vs. $1/[4\text{-CP}]_0$ at 30 and 60 °C, indicating that the k_{obsd} value is independent of temperature whereas the K_{ads} value decreases at higher temperature. These results are reasonable because all variables included in k_{obsd} are hardly dependent of temperature and higher temperature enhances the desorption of the adsorbed 4-CP. This fact also supports the validity of the rate law (16).

3.6. Formation of byproducts

GC/MS measurements demonstrated the formation of p-benzoquinone (BQ) and hydroquinone (HQ) as the intermediates. Fig. 12 shows the variation in the concentration of 4-CP, BQ, HQ and TOC during the irradiation of 390 min. The degradation of 4-CP was accomplished at the irradiation of 150 min and the formation of BQ and HQ was not detected after the irradiation of 330 min. It is noted that 90.7% of 4-CP was completely mineralized at the irradiation of 390 min.

4. Conclusion

We successfully prepared porous Pt-TiO_2 with the BET surface area higher than 200 m^2 g^{-1} by the sol–gel method involving dialysis and demonstrated the superior photocatalytic activity under both UV and VL irradiation. Various metal-ion-doped TiO_2 have been prepared by standard sol–gel methods consisting of stirring, evaporating and sintering. This study clearly demonstrates that dialysis process leads to the formation of mesopores, which is responsible for the increase in the surface area of Pt-TiO_2. Furthermore, during the dialysis, Cl^- and NO_3^- ions were removed whereas most of Pt ion was remained in the sol. The removal of Cl^- is beneficial because of inhibition of the formation of harmful chlorinated compounds during calcination. We also performed the kinetic studies and obtained the reaction rate law under VL irradiation. Photocatalysts acting under VL are required to utilize effectively the solar energy. Although BQ and HQ were detected as intermediates, 90.7% of 4-CP was completely mineralized at the irradiation for 390 min. Since phenolic compounds like 4-CP has been known to form the surface complexes with TiO_2, we are currently investigating the visible activity of Pt-TiO_2 for the chlorinated compounds without the phenolic moiety.

Acknowledgments

This work was supported by Strategic Research Program of Yamaguchi University (2011). We thank the Center for Instrumental Analysis at Yamaguchi University for the ICP measurements.

References

[1] D.F. Ollis, H. Al-Ekabi (Eds.), Photocatalytic Purification and Treatment of Water and Air, Elsevier, Amsterdam, 1993.
[2] M.R. Hoffmann, S.T. Martin, W. Choi, D.W. Bahnemann, Chem. Rev. 95 (1995) 69–96.
[3] A. Fujishima, T.N. Rao, D.A. Tryk, J. Photochem. Photobiol. C: Rev. 1 (2000) 1–21.
[4] U.I. Gaya, A.H. Abdullah, J. Photochem. Photobiol. C: Rev. 9 (2008) 1–12.
[5] B. Ohtani, J. Photochem. Photobiol. C: Rev. 11 (2010) 157–178.
[6] A. Fujishima, X. Zhang, D.A. Tryk, Surf. Sci. Rep. 63 (2008) 515–582.
[7] R. Asahi, T. Morikawa, T. Ohwaki, K. Aoki, Y. Taga, Science 293 (2001) 269–271.
[8] H. Irie, Y. Watanabe, K. Hashimoto, Chem. Lett. 32 (2003) 772–773.
[9] T. Umebayashi, T. Yamaki, S. Yamamoto, A. Miyashita, S. Tanaka, T. Sumita, K. Asai, J. Appl. Phys. 93 (2003) 5156–5160.
[10] L. Lin, W. Lin, Y. Zhu, B. Zhao, Y. Xie, Chem. Lett. 34 (2005) 284–285.
[11] W. Zhao, W. Ma, C. Chen, J. Zhao, Z. Shuai, J. Am. Chem. Soc. 126 (2004) 4782–4783.
[12] J. Wang, D.N. Tafen, J.P. Lewis, Z. Hong, A. Manivannan, M. Zhi, M. Li, N. Wu, J. Am. Chem. Soc. 131 (2009) 12290–12297.
[13] H. Irie, Y. Watanabe, K. Hashimoto, J. Phys. Chem. B 107 (2003) 5483–5486.
[14] X. Zhang, L. Lei, Mater. Lett. 62 (2008) 895–897.
[15] S. Klosek, D. Raftery, J. Phys. Chem. B 105 (2001) 2815–2819.
[16] J.C.-S. Wu, C.-H. Chen, J. Photochem. Photobiol. A: Chem. 163 (2004) 509–515.
[17] D.H. Kim, K.S. Lee, Y.-S. Kim, Y.-C. Chung, S.-J. Kim, J. Am. Ceram. Soc. 89 (2006) 515–518.
[18] S. Kim, S.-J. Hwang, W. Choi, J. Phys. Chem. B 109 (2005) 24260–24267.
[19] J. Choi, M.R. Hoffmann, J. Mater. Res. 25 (2010) 149–158.
[20] J. Choi, H. Park, M.R. Hoffmann, J. Phys. Chem. C 114 (2010) 783–792.
[21] Q. Xu, M.A. Anderson, J. Mater. Res. 6 (1991) 1073–1081.
[22] S. Yamazaki, K. Ichikawa, A. Saeki, T. Tanimura, K. Adachi, J. Phys. Chem. A 114 (2010) 5092–5098.
[23] S. Yamazaki, T. Tanimura, A. Yoshida, K. Hori, J. Phys. Chem. 108 (2004) 5183–5188.
[24] T. Tanimura, A. Yoshida, S. Yamazaki, Appl. Catal. B: Environ. 61 (2005) 346–351.
[25] S. Yamazaki, H. Tsukamoto, K. Araki, T. Tanimura, I. Tejedor-Tejedor, M.A. Anderson, Appl. Catal. B: Environ. 33 (2001) 109–117.
[26] J. Lee, W. Choi, J. Phys. Chem. B 109 (2005) 7399–7406.
[27] S.F. Chin, S.C. Pang, M.A. Anderson, Mater. Lett. 64 (2010) 2670–2672.
[28] C. Xi, Z. Chen, Q. Li, Z. Jin, J. Photochem. Photobiol. A: Chem. 87 (1995) 249–255.
[29] R.D. Shannon, Acta Cryst. A32 (1976) 751–767.
[30] S. Kim, W. Choi, J. Phys. Chem. B 109 (2005) 5143–5149.
[31] U. Stafford, K.A. Gray, P.V. Kamat, A. Varma, Chem. Phys. Lett. 205 (1993) 55–61.
[32] S.T. Martin, J.M. Kesselman, D.S. Park, N.S. Lewis, M.R. Hoffmann, Environ. Sci. Technol. 30 (1996) 2535–2542.
[33] A. Orlov, D.J. Watson, F.J. Williams, M. Tikhov, R.M. Lambert, Langmuir 23 (2007) 9551–9554.
[34] J.-W. Kang, M.R. Hofmann, Environ. Sci. Technol. 32 (1998) 3194–3199.